Optimal fiber content and distribution in fiber-reinforced solids using a reliability and NURBS based sequential optimization approach

Hamid Ghasemi[1], Roberto Brighenti[2], Xiaoying Zhuang*[3], Jacob Muthu[4],Timon Rabczuk*[1, 5]

[1] Institute of Structural Mechanics, Bauhaus University Weimar (BUW), Marienstraße 15, 99423 Weimar, Germany
[2] Dep. of Civil Eng, Env. & Architect. , U of Parma, Parco Area delle Scienze, 181/A, 43100 Parma, Italy
[3] Dep. of Geotech. Eng., College of Civil Eng., Tongji Uni., 1239 Siping Road, Shanghai 200092, China
[4] School of Mechanical, Industrial and Aeronautical Eng., U. of the Witwatersrand, WITS 2050, S. Africa
[5] Professor at BUW and School of Civil, Environmental and Architectural Eng., Korea University, Seoul, S. Korea

Abstract

A double stage sequential optimization algorithm for finding the optimal fiber content and its distribution in solid composites, considering uncertain design parameters, is presented. In the first stage, the optimal amount of fiber in a Fiber Reinforced Composite (FRC) structure with uniformly distributed fibers is conducted in the framework of a Reliability Based Design Optimization (RBDO) problem. In the second stage, the fiber distribution optimization having the aim to more increase in structural reliability is performed by defining a fiber distribution function through a Non-Uniform Rational B-Spline (NURBS) surface. The output of stage 1(optimal fiber content for homogeneously distributed fibers) is considered as the input of stage 2. The output of stage 2 is Reliability Index (RI) of the structure with optimal fiber content and optimal fiber distribution. First order reliability method in order to approximate the limit state function and a homogenization approach, based on the assumption of random orientation of fibers in the matrix, are implemented. The proposed combined model is able to capture the role of available uncertainties in FRC structures through a computationally efficient algorithm using all sequential, NURBS and sensitivity based techniques. Performed case studies show as an increase in model uncertainties yields to structural unreliability. Moreover, when system unreliability increases fiber distribution optimization becomes more influential.

Keywords: Reliability Based Design Optimization (RBDO), Reliability Analysis, Fiber Reinforced Composite (FRC), Fiber Distribution Optimization, NURBS

1. Introduction

Uniform mechanical properties of FRCs depend on uniform dispersion of fibers in the matrix.

* Corresponding authors. Address: Institute of Structural Mechanics, Bauhaus University Weimar, Marienstraße 15, 99423 Weimar, Germany (T. Rabczuk). Tel.: +49 3643 584511. E-mail addresses: timon.rabczuk@uni-weimar.de xiaoyingzhuang@tongji.edu.cn (X. Zhuang)

Nomenclature of homogenization technique:

$\boldsymbol{C_f(x), C_m(x)}$	Elastic tensor of the fiber and of the matrix material, respectively
$\boldsymbol{C_{eq}}$	Homogenized elastic tensor of the composite
$\boldsymbol{E_f, E_m}$	Young's modulus of the fiber phase and of the matrix, respectively
$\boldsymbol{i}$	Unit vector parallel to the generic fiber axis
$\boldsymbol{Q = (i \otimes i)}$	Second-order tensor related to the fiber lying along the $\boldsymbol{i}$ direction
$\boldsymbol{V, V_m, V_f}$	Volume of the composite, volume of the matrix phase and volume of the fiber fraction present in the RVE, respectively
$\boldsymbol{w'}$	Composite work rate
$\boldsymbol{x}$	Generic position vector
$\boldsymbol{\varepsilon, \dot{\tilde{\varepsilon}}}$	Strain and virtual strain rate tensors, respectively
$\boldsymbol{\varepsilon_f, \widetilde{\varepsilon_f}, \dot{\widetilde{\varepsilon}}_f}$	Fiber strain, virtual strain and virtual strain rate, respectively
$\boldsymbol{\kappa(x)}$	Point function denoting the presence of the matrix at the location **x**
$\boldsymbol{\chi(x)}$	Point function denoting the presence of the fiber at the location **x**
$\boldsymbol{\mu = \frac{V_m}{V}}$	RVE matrix volume fraction
$\boldsymbol{\eta_p = \frac{V_f}{V}}$	RVE fiber volume fraction
$\boldsymbol{\sigma, \sigma_f, \sigma_{eq}}$	Stress in composite, axial stress in a fiber and in the equivalent material

Many efforts have been made to quantify, improve and inspect uniform dispersion of reinforcing elements in the matrix phase [1-6]. In contrary, few researches have been done to obtain non-uniform distribution of fibers in order to obtain optimal structural response. Huang and Haftka [7] tried to optimize fiber orientation (not distribution) near a hole in a single layer of multilayer composite laminates in order to increase the load caring capacity by using Genetic Algorithm (GA). Optimal distribution of the fibers in a FRC structure has been presented in [8] and [9] by using GA and sensitivity based approaches, respectively. The optimal fiber content and also available uncertainties are addressed neither in [8] nor [9].

Actual characteristics of a FRC material are influenced by many of uncertainties which come from variety of sources such as constituent material properties, manufacturing and process imperfections, loading / boundary conditions or even structural geometry. Neglecting the role of these uncertainties may affect the reliability of the structure. Structural reliability can be defined as the ability of a structure to fulfill some sought design purposes. In order to quantify these design purposes, limit state concept has been introduced to obtain a quantitative measure for

structural safety. Deterministic limit states without considering uncertainties can be unreliable and might bring to overestimate the bearing capacity of the structure, with the risk of its catastrophic failure. However, the traditional approach which is based on safety factor is not always efficient and could result in a costly and unnecessary conservatism [10].

There are some methods for considering the role of uncertainties in design performance. One of these methods is the so-called RBDO which tries to find optimal performance considering some probabilistic design constraints. Motivated by capabilities of RBDO in uncertainty quantification, some researchers have implemented it in the design of composite structures. Though there are some exceptions, most of these researches are related to composite laminates. However, to the knowledge of the authors, the solid FRC structures are not thoroughly explored. Thanedar and Chamis [11] developed a procedure for the tailoring of layered composite laminates subjected to probabilistic constraints and loads. The work of Jiang et al. [12] suggested a methodology to optimize the plies orientations of a composite laminated plate having uncertain material properties. Gomes and his coworkers [13] addressed the problem of composite laminate optimization by using GA and Artificial Neural Networks (ANN); while Antonio's work [14] presented reliability based robust design optimization methodology. Noh et al. [15] have implemented RBDO methodology for purpose of optimizing volume fraction in a Functionally Graded Material (FGM) laminate composite.

Generally, increasing the fiber volume fraction in a FRC composite will increase its structural strength and stiffness. However the existence of a practical upper limit should be considered. Normally, composite structural elements under mechanical actions have some regions which are on the edge of design constraints (e.g. the maximum allowable stress is exceeded) and can be identified as failure zones. Usually these failure zones dictate the required content of the reinforcing element in order to get a properly strengthened overall structure, fulfilling everywhere the design constraints. Considering uniform distribution of fibers through the structure, initially safe regions that already fulfill the design constraints will inevitably increase their fiber content. Thus, an efficient optimization approach which seeks towards optimal fiber content should also pay attention to optimal distribution of fibers in order to strengthen only those portions of the structure (failure zones) for which it is necessary to improve their bearing capacity. From the above discussions it appears that the joint manipulation of these two parameters (i.e. fiber content and its distribution) while available uncertainties are also

addressed, will be a necessary approach towards more efficient and reliable structural optimization. Such an approach could obviously have promising industrial application such as patch repair optimization in cracked plates [16-18] and minimizing stress concentration in sandwich beams [15]. It can also be extended to cement composites [19-20].

The outline of the present paper is as follows: Section 2 presents an overview of homogenization technique for obtaining equivalent material property while a description of reliability analysis and RBDO is presented in Section 3. Section 4 briefly describes fiber distribution optimization procedure followed by the presentation of sequential optimization methodology which is discussed in more details in Section 5. Section 6 contains some numerical examples. The concluding remarks are presented in Section 7.

2. FRC homogenization methodology

Basically, the aim of homogenization techniques is to find equivalent material characteristics in a Representative Volume Element (RVE) of composite material. There are some classical approaches in order to model the material properties of a composite material among which are the Rule of Mixture, Hashin-Shtrikman type bounds [21, 22], Variational Bounding Techniques [23], Self Consistency Method [24] and Mori-Tanaka Method [25]. The homogenization approach used in this research work is a simplified version of a recently developed mechanical model to get the FRC constitutive behavior based on energetic equivalence between the real FRC material and the macroscopically homogeneous one. This is evaluated through the evolution of the shear stress distribution along the fiber-matrix interface during the loading process. The adopted model for fiber homogenization can be considered to be mechanically-based, since the fiber contribution to the FRC mechanical properties are determined from the effective stress transfer between matrix and fibers. The possibility of fiber-matrix debonding can be easily taken into account [8, 26]. Since the goal of this paper is to focus on fiber content and distribution through the structure rather than developing micromechanical model, for the sake of simplicity, we neglect this issue in the present work. It can be stated that for not too high stressed composite elements (as followed in our numerical examples) leading to shear fiber-matrix interface stresses well below the allowable limit shear bimaterial stress, the debonding phenomenon can reasonably assumed not to occur. Fiber failure is also neglected. This approach is briefly summarized below; however interested reader can refer to [27-29] for more details.

The equivalent elastic properties of a fiber reinforced composite material – for which the hypotheses of short, homogeneously and randomly dispersed fibers are made – can be obtained by equating the virtual work rate of constituents for a RVE of the composite material (Fig.1) with equivalent homogenized one as shown by:

$$w' = \overbrace{\int_V \kappa(\boldsymbol{x})\, \dot{\tilde{\boldsymbol{\varepsilon}}} : \boldsymbol{\sigma} dV + \int_V \chi(\boldsymbol{x})\, \dot{\tilde{\boldsymbol{\varepsilon}}}_f : \boldsymbol{\sigma}_f\, dV}^{composite's\ work\ rate} = \overbrace{\int_V \dot{\tilde{\boldsymbol{\varepsilon}}} : \boldsymbol{\sigma}_{eq} dV}^{homogenized\ material's\ work\ rate} \tag{1}$$

where $\dot{\tilde{\boldsymbol{\varepsilon}}}_{\mathrm{f}}$, $\boldsymbol{\sigma}_{\mathrm{f}}$ are the virtual strain rate and the stress in a fiber, respectively, while the scalar functions $\kappa(\mathbf{x})$ and $\chi(\mathbf{x})$ assume the following meanings:

$$\kappa(\boldsymbol{x}) = \begin{cases} 1 & if\ (\boldsymbol{x}) \in V_m \\ 0 & if\ (\boldsymbol{x}) \notin V_m \end{cases} \quad \text{and} \quad \chi(\boldsymbol{x}) = \begin{cases} 1 & if\ (\boldsymbol{x}) \in V_f \\ 0 & if\ (\boldsymbol{x}) \notin V_f \end{cases} \tag{2}$$

and allow us to identify the location of the material point $\boldsymbol{x}$ either in the matrix or in the reinforcing phase.

The constitutive relationships of the fibers and of the bulk material can be simply expressed through the following linear relations:

$$\boldsymbol{\sigma}_f = E_f \cdot (\boldsymbol{i} \otimes \boldsymbol{i}) : \boldsymbol{\varepsilon} \quad \text{and} \quad \boldsymbol{\sigma}_{eq}(\boldsymbol{x}) = \boldsymbol{C}_{eq}(\boldsymbol{x}) : \boldsymbol{\varepsilon} \tag{3}$$

in which E_f is the fibers' Young's modulus, $\boldsymbol{\varepsilon}_f$ is the fiber strain, $\boldsymbol{C}_{eq}$ is the composite equivalent elastic tensor while $\boldsymbol{\varepsilon}$ is the actual matrix strain tensor. Eq. (3) has been written by taking into account that the matrix strain measured in the fiber direction is given by $\boldsymbol{\varepsilon}_f = (\boldsymbol{i} \otimes \boldsymbol{i}) : \boldsymbol{\varepsilon}$ where $\boldsymbol{i} = (sin\theta cos\phi\ \ sin\theta sin\phi\ \ cos\theta)$ is the unit vector identifying the generic fiber direction, (Fig.1); and analogously for the virtual $\tilde{\boldsymbol{\varepsilon}}_{\mathbf{f}}$ and the virtual strain rate,

$$\tilde{\boldsymbol{\varepsilon}}_f = (\boldsymbol{i} \otimes \boldsymbol{i}) : \tilde{\boldsymbol{\varepsilon}} \quad \text{and} \quad \dot{\tilde{\boldsymbol{\varepsilon}}}_f = (\boldsymbol{i} \otimes \boldsymbol{i}) : \dot{\tilde{\boldsymbol{\varepsilon}}} \tag{4}$$

by substituting the above expressions in the virtual work rate equality (Eq. (1)) we can finally identify the composite equivalent elastic tensor:

$$\boldsymbol{C}_{eq}(\boldsymbol{x}) = \frac{1}{V} \int_V \{\kappa(\boldsymbol{x}) \cdot \boldsymbol{C}_m + \chi(\boldsymbol{x}) E_f \cdot [\boldsymbol{Q} \otimes \boldsymbol{Q}]\} dV =$$

$$= \mu \cdot \boldsymbol{C}_m + \eta_p E_f \cdot \int_V \boldsymbol{Q} \otimes \boldsymbol{Q}\, dV \tag{5}$$

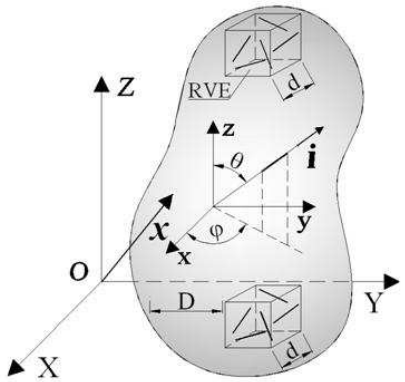

Fig.1. Fiber reinforced composite material: definition of the RVE (with a characteristic length d, while the composite has a characteristic length D>>d) and of the fiber orientation angles φ, θ, ref. [26].

where the second-order tensor $\boldsymbol{Q} = (\boldsymbol{i} \otimes \boldsymbol{i})$ has been introduced and the matrix and fiber volume fractions $\mu = \frac{1}{V} \int_V \kappa(\boldsymbol{x})\, dV = \frac{V_m}{V}$ and $\eta_p = \frac{1}{V} \int_V \chi(\boldsymbol{x})\, dV = \frac{V_f}{V}$ have been used.

It can be easily deduced as the equivalent material is macroscopically homogeneous at least at the scale of the RVE with the volume V. So, the equivalent elastic tensor $\boldsymbol{C}_{eq}(\boldsymbol{x})$ does not depend on the position vector, i.e. $\boldsymbol{C}_{eq}(\boldsymbol{x}) = \boldsymbol{C}_{eq}$.

The calculation of the equivalent elastic tensor $\boldsymbol{C}_{eq}$ through Eq. (5), needs to evaluate the below integral over a sufficiently large volume, representative of the macroscopic characteristics of the composite. The above integral can be suitably assessed on a hemisphere volume which allows considering all possible fiber orientations in the composite:

$$\frac{1}{V_{hem}} \int_{V_{hem}} \boldsymbol{Q} \otimes \boldsymbol{Q} dV = \int_0^R \int_0^{2\pi} \int_0^{\pi/2} (\boldsymbol{Q} \otimes \boldsymbol{Q}) r\, d\phi\, r \sin\theta\, d\theta\, dr =$$

$$= \frac{R^3}{3} \frac{1}{\frac{2\pi R^3}{3}} \int_0^{2\pi} \int_0^{\pi/2} (\boldsymbol{Q} \otimes \boldsymbol{Q}) d\phi\ \sin\theta\ d\theta$$

$$= \frac{1}{2\pi} \int_0^{2\pi} \int_0^{\pi/2} (\boldsymbol{Q} \otimes \boldsymbol{Q}) d\phi\ \sin\theta\ d\theta \qquad (6)$$

3. Reliability assessment and optimization formulations (stage-1)

The fundamentals of structural reliability are briefly presented below however, interested readers can refer to [30] and references therein for more details. The structural reliability concept

can be simply described by the example of a steel rod with constant cross sectional area under uniaxial tension (see Fig. 2). In the deterministic case, if the applied load (L) is less than rod strength (R), failure will not occur and the rod will be safe and the conventional safety factor index ($S.F = \frac{R}{L}$) is used to quantify the system level of confidence. In probabilistic case, L and R are not fixed values but instead they are random variables containing uncertainties. In this case $\boldsymbol{X}_L$ and $\boldsymbol{X}_R$ are nonnegative independent random variables with Probability Density Functions (PDF) $f_L(x_L)$ and $f_R(x_R)$, respectively. In essence, for a vector of random variables $\boldsymbol{X} = \{x_1, \dots, x_n\}^T$, the PDF can be calculated by $f_{\boldsymbol{X}}(x) = \frac{d}{dx} F_{\boldsymbol{X}}(x)$, where $F_{\boldsymbol{X}}(x)$ is the so called Cumulative Distribution Function (CDF) and relates the probability of a random event to a prescribed deterministic value x, (i.e. $F_{\boldsymbol{X}}(x) = Prob[\boldsymbol{X} < x]$).

In considering the rod example, the boundary between safe (i.e. $x_R > x_L$) and failure (i.e. $x_R < x_L$) regions can be defined by $g(x) = x_R - x_L$ which is called Limit State Function (LSF). Thus, $g(x) \leq 0$ denotes a subset of the space, where failure occurs.

The concept of Reliability Index (β) which has been proposed by Hasofer and Lind [31] in 1974 requires standard normal non-correlated variables; so the transformations from correlated non-Gaussian variables $\boldsymbol{X}$ to uncorrelated Gaussian variables $\boldsymbol{U}$ (with zero means and unit standard deviations) is needed. According to this definition of β, the design point is chosen such as to maximize the PDF within the failure domain. Geometrically, it corresponds to the point in failure domain having the shortest distance from the origin of reduced variables to the limit state surface (i.e. $g(\boldsymbol{U}) = 0$, as shown in Fig.2). Mathematically, it is a minimization problem with an equality constraint:

$$\begin{cases} \beta = min(\boldsymbol{U}.\boldsymbol{U}^T)^{\frac{1}{2}} \\ s.t: \\ g(\boldsymbol{U}) = 0 \end{cases} \tag{7}$$

which leads to the Lagrange-function:

$$L = \min \{\frac{1}{2}\boldsymbol{U}^T\boldsymbol{U} + \lambda g(\boldsymbol{U})\} \tag{8}$$

The solution of Eq. (8) is called the Most Probable Point (U_{MPP}) or briefly *MPP* and can be obtained by a standard optimization solver.

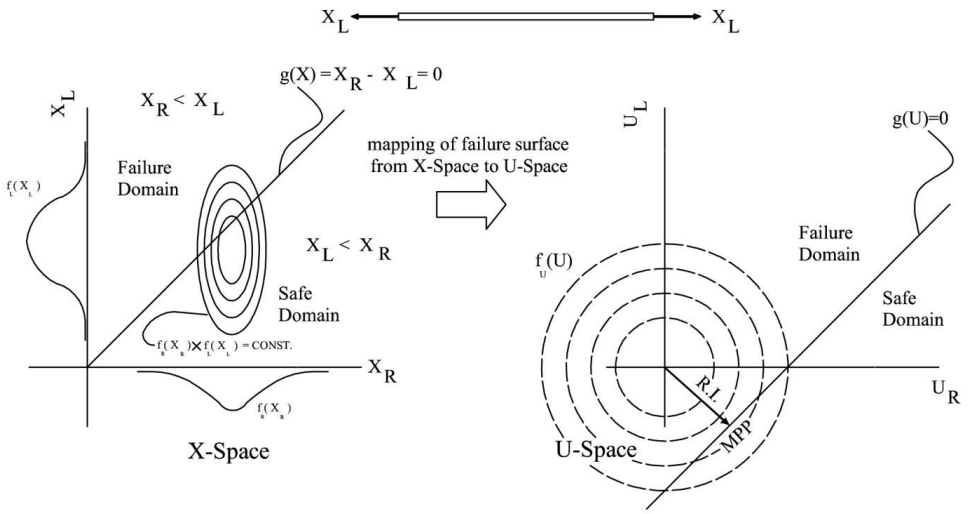

Fig.2. Structural reliability concept

The failure probability, P_f, can be measured by the probability integral as:

$$P_f = Prob[g(x) \leq 0] = \int_{x|g(x)\leq 0} f_{\boldsymbol{X}}(x)dx \tag{9}$$

The evaluation of the integral in Eq. (9) (the fundamental equation of reliability analysis) in most cases is not an easy task and needs specific solution techniques. One approach is to analytically approximate this integral, in order to get simpler functions for P_f. Such techniques can be categorized into two major groups: First and Second Order Reliability Method (FORM & SORM) which respectively approximate LSF with the first order and the second order of Taylor expansion at the MPP (Fig. 3).

There are also alternative methods for calculating the probability integral: among them Monte-Carlo Method (MCM) may be the most important one since it is usually used as the reference method due to its precision to calculate failure probability. Each of the above cited methods has advantages and disadvantages which should be considered precisely before implementation. For instance even though MCM is a precise method, it shows a serious drawback in the case of small values of the failure probability [32]. Computational cost is another dominant parameter for selecting the appropriate solution method. Methods based on the SORM and MCM approaches are usually numerically more expensive in comparison with FORM. In practical problems an appropriate balance must be necessarily considered between accuracy and cost of the analysis. In the present work FORM has been implemented since it is suitable for cases with a small number

of random variables. Such an approach is usually sufficiently accurate to be used for real applications of structural design [33]. In the following, the implementation of the FORM is briefly described, however more details about available methods for structural reliability analysis can be found in [32].

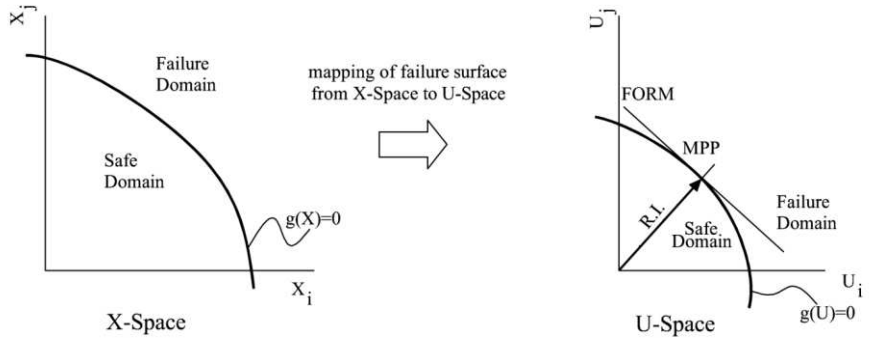

Fig.3. Graphical representation of the FORM approximation

3.1. First order reliability method (FORM)

The FORM approximation can be traced back to First Order Second Moment (FOSM) method which is based on first order Taylor series approximation of the LSF, linearized at the mean values of random variables, while a Second-Moment statistics (means and covariances) is used. In this context the limit state function can be approximated as below:

$$g(x) = g(x_0) + \sum_{i=1}^{n} \frac{\partial g}{\partial x_i}|_{x=x_0}(x_i - x_{i0}) + \frac{1}{2}\sum_{i=1}^{n}\sum_{k=1}^{n} \frac{\partial^2 g}{\partial_{x_i}\partial_{x_k}}|_{x=x_0}(x_i - x_{i0})(x_k - x_{k0}) + \cdots \tag{10}$$

Terminating the series after the linear terms yields:

$$\mathbb{E}[Z] = \mathbb{E}[g(\boldsymbol{X})] = g(x_0) + \sum_{i=1}^{n} \frac{\partial g}{\partial x_i}\mathbb{E}[x_i - x_{i0}] \tag{11}$$

where $\mathbb{E}$ stands for expected value (or ensemble average) of a random quantity $g(\boldsymbol{X})$ and can be defined in terms of the probability density function of x as:

$$\mathbb{E}[g(\boldsymbol{X})] = \int_{-\infty}^{+\infty} g(x) f_X(x) dx \tag{12}$$

If the mean value vector $\bar{\boldsymbol{X}}$ is chosen as the starting expansion point x_0 for the Taylor series, then $\mathbb{E}[Z] = g(x_0)$ and the variance becomes:

$$\sigma_Z^2 = \mathbb{E}[(Z-\bar{Z})^2] = \mathbb{E}[(g(\boldsymbol{X}) - g(\bar{\boldsymbol{X}}))^2] = \mathbb{E}\left[\left(\sum_{i=1}^{n} \frac{\partial g}{\partial X_i}(X_i - \bar{X}_i)\right)^2\right]$$

$$= \sum_{i=1}^{n}\sum_{k=1}^{n} \frac{\partial g}{\partial x_i}\frac{\partial g}{\partial x_k}\mathbb{E}[(X_i - \bar{X}_i)(X_k - \bar{X}_k)] \tag{13}$$

finally the distribution function $F_Z(z)$ is approximated by a normal distribution:

$$F_Z(z) = \Phi\left(\frac{z-\bar{Z}}{\sigma_Z}\right) \tag{14}$$

then we obtain the approximate result:

$$P_f = F_Z(0) = \Phi\left(-\frac{\bar{Z}}{\sigma_Z}\right) \tag{15}$$

the reliability R can finally be expressed as:

$$R = \Phi(\beta) \tag{16}$$

where $\beta = \frac{\bar{Z}}{\sigma_Z}$ and the probability of failure consequently becomes expressed as:

$$P_f = 1 - R = 1 - \Phi(\beta) = \Phi(-\beta) \tag{17}$$

3.2. RBDO

In its basic form the problem of RBDO can be expressed as below:

$$\min_{\boldsymbol{\theta}} C(\boldsymbol{\theta})\ s.t.\ \begin{vmatrix} f_1(\boldsymbol{\theta}), \dots, f_{q-1}(\boldsymbol{\theta}) \le 0 \\ f_q(\boldsymbol{X}, \boldsymbol{\theta}) = \beta_t - \beta(\boldsymbol{X}, \boldsymbol{\theta}) \le 0 \end{vmatrix} \tag{18}$$

where $\boldsymbol{\theta}$ is the vector of the design variables, $C(\boldsymbol{\theta})$ is the cost or objective function, $f_1(\boldsymbol{\theta}), \dots, f_{q-1}(\boldsymbol{\theta})$ is a vector of 1 to $(q-1)$ deterministic constraints over the design variables $\boldsymbol{\theta}$, $f_q(\boldsymbol{X}, \boldsymbol{\theta})$ is the reliability constraint enforcing the respect of LSF and considering the uncertainty to which some of the model parameters $\boldsymbol{X}$ are subjected to. β_t is the target safety index. To solve Eq. (18), the open source software FERUM 4.1 [34] has been implemented and linked to FE code which evaluates the LSF.

In our model, $\boldsymbol{\theta}$ could be defined as the matrix or fiber Young's modulus, material density or applied loads while the objective function corresponds to find the optimal fiber volume fraction. Without loss in generality, the maximum deflection (d_{max}) of the component under the applied load (obtained by FEM code) is compared with predetermined value (d_{all}) as design constraint.

The limit state function is defined by $g(x) = d_{all} - d_{max}$ and the failure ($g(x) \leq 0$) occurs when $d_{all} \leq d_{max}$. It is straightforward to extend design constraints to other structural response like maximum stress, maximum stress mismatch or even to thermal and electrical fields. However, as the aim of this paper is introducing the sequential approach in optimizing FRC structures, we neglect to discuss about them for sake of simplicity and clarity.

4. Deterministic fiber distribution optimization using NURBS functions (stage-2)

Currently, NURBS are incorporated into most of the geometric modeling systems. NURBS functions are used within this work to calculate an approximation of a given set of points through a smooth function. There are two notions of meshes: the control mesh and the physical mesh. The former is defined by control points and is like a scaffold that controls the geometry, while the latter defines the actual geometry. There are also two notions of elements used in the physical mesh that must be taken into account: the patch and the knot span. The patch is a sub-domain and is represented in either parent domain or physical space while knot spans (bonded by knots) define each patch. Based on the topology, knots can be points, lines or surfaces. Since NURBS curves and surfaces are exhaustively presented in numerous references, to prevent duplication, interested readers are referred to [35] to find more about NURBS surface characteristics. Fig.4 schematically shows different NURBS spaces and approximation of nodal values by a smooth function.

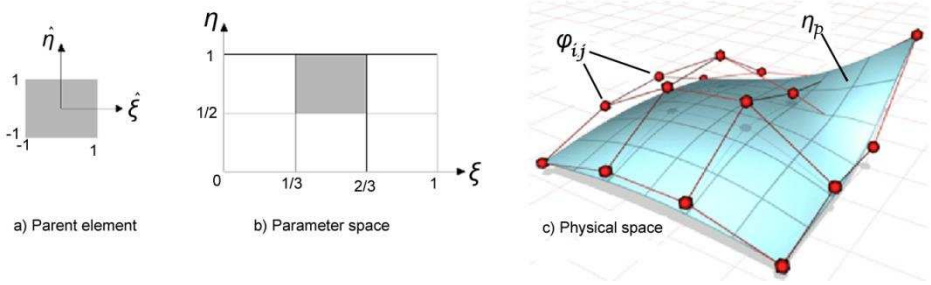

Fig.4. Different NURBS domains (a), (b), (c) and approximation by NURBS function (c)

It should be declared that NURBS basis functions have dual applications in the present work: the model analysis and fiber distribution. The former is performed by quadratic NURBS finite elements through an isogeometric analysis (IGA) approach [35] while the latter is presented in more detail in [9] and is briefly described in following.

In our methodology nodal fiber volume fraction ($\varphi_{i,j}$) on control points are defined as design variables and fiber distribution (η_p) is approximated by using NURBS surface. Every point on parametric mesh space of the design domain is mapped to geometrical space having two attributes, geometrical coordinates and fiber volume fraction value. Due to intrinsic characteristics of NURBS (higher order basis and compact support, see [35]), even using coarse meshes, fiber distribution function described through a NURBS surface is smooth enough to have a clear representation of optimization results with no need for any further image processing techniques.

Fiber distribution function $\eta_p(\boldsymbol{x},\boldsymbol{y})$, which indicates the fiber amount at every design point and is used for obtaining homogenized mass and stiffness of finite elements, is defined according to:

$$\eta_p(\boldsymbol{x},\boldsymbol{y}) = \sum_{i=1}^{n}\sum_{j=1}^{m} R_{i,j}^{p,q}(\xi,\eta)\ \varphi_{i,j} \tag{19}$$

where $R_{i,j}^{p,q}$ are NURBS basis functions. Once the fiber volume fraction at each point is available, by substitution in Eq. (5), we can define the equivalent mechanical characteristics of the domain through the equations below:

$$\boldsymbol{C}_{eq}(\boldsymbol{x},\boldsymbol{y}) = \left(1-\eta_p\right)\cdot \boldsymbol{C}_m + \eta_p E_f \cdot \int_V \boldsymbol{Q}\otimes\boldsymbol{Q}\ dV \tag{20}$$

In deterministic fiber distribution optimization problem, minimization of strain energy is considered as objective function. For the problem with m load cases we have:

$$U = \sum_{i=1}^{m} \lambda_i U^i \quad \lambda_i > 0 \tag{21}$$

where U and U^i are the total strain energy and elastic strain energy for i^{th} load case, respectively. λ_i is the associated weight for strain energy which has been considered equal to unity unless otherwise specified. The terms U^i can be also defined as:

$$U^i = [\sum_{e=1}^{nel} \frac{1}{2}\int_V \boldsymbol{\varepsilon}_e^T\, \boldsymbol{C}_{eq}\, \boldsymbol{\varepsilon}_e dV]^i \tag{22}$$

in Eq. (22) $\boldsymbol{\varepsilon}_e$ is the strain vector associated with element e and $\boldsymbol{C}_{eq}$ is the homogenised elastic tensor of the composite at each point evaluated according to Eq. (5). nel is the number of elements in the FE model.

The optimization problem can be finally summarized as follows:

Minimize: U

Subjected to:

$$w_f = \int_V \eta_p \rho_f \, dV \leq w_{f0} \tag{23}$$

$$\boldsymbol{K}\boldsymbol{u} = \boldsymbol{f} \tag{24}$$

$$\varphi_{i,j} - 1 \leq 0 \tag{25}$$

$$-\varphi_{i,j} \leq 0 \tag{26}$$

where w_f is the total fiber weight in every optimization iteration and w_{f0} is an arbitrary initial fiber weight which must be set at the beginning of the optimization process. $\boldsymbol{K}$, $\boldsymbol{u}$ and $\boldsymbol{f}$ in Eq. (24) which represents the general system of equilibrium equations in linear elastic finite elements method, represent the global stiffness matrix of the system, the displacement and force vector, respectively.

By introducing a proper Lagrangian objective function, l, and by using the Lagrangian multipliers method we have:

$$l = U - \left(w_f - w_{f0}\right) - \sum_{i,j=1}^{ncp} \psi_1\left(\varphi_{i,j} - 1\right) - \sum_{i,j=1}^{ncp} \psi_2\left(-\varphi_{i,j}\right) \tag{27}$$

where ψ_1, ψ_2 are upper and lower bounds values of the Lagrange multipliers, respectively. ncp is the number of control points. By equating the first derivative of Eq. (27) to zero we will obtain:

$$\frac{\partial l}{\partial \varphi_{i,j}} = \frac{\partial U}{\partial \varphi_{i,j}} - \frac{\partial w_f}{\partial \varphi_{i,j}} - \psi_1 + \psi_2 = 0 \tag{28}$$

In this work we have implemented optimality criteria (OC) based optimization (Zhou & Rozvany, 1991, [36]) to numerically solve Eq. (28). OC represents a simple tool to be implemented and allows a computationally efficient solution because each design variable is updated independently. A detailed description of the updating scheme of OC is not reported in the paper; however interested readers can refer to [36] for more details.

5. Double sequential stages optimization procedure

The sequential optimization algorithm is schematically illustrated in Fig. 5. In this approach there are two successive optimization stages. Stage 1 includes a stochastic fiber content optimization algorithm and stage 2 includes a fiber distribution optimizer. In the first stage, based on the nature of the problem, the designer can decide which parameters would be

deterministic and which ones probabilistic. He can also set the initial values of the parameters, variables and solution settings. Traditional RBDO is implemented by use of a nested or double loop approach. In this method, each step of the iteration for design optimization involves another loop of iteration for reliability analysis (i.e. FORM). In this stage, minimization of fiber content is considered as optimization objective function and after convergence, the output is used as the input for the second stage. In the second stage, NURBS finite elements which are implemented and used for domain discretization, define continuous and smooth mesh independent fiber distribution function by using the nodal volume fractions of fibers as the optimization design variables. The second stage is initialized by using the fiber volume fraction value, coming as stage 1. Afterwards Optimality Criteria (OC) updates design variables. This computational procedure is executed iteratively, till no sensible changes occur in design variables [9].

In the presented model, two separate reliability indices ($\beta_1$and β_2) are introduced: β_1 is the first stage reliability index (which is used for obtaining optimal fiber volume fraction through the RBDO in stage 1) and the second reliability index, β_2, is the target reliability index of the final optimized structure. β_2 represents the reliability index of the structure after fiber distribution optimization. β_1 is the model input (set by designer at the first run of the algorithm) while β_2 is the output of the model. Clearly, $\beta_1 < \beta_2$ because it is supposed that fiber distribution optimization increases the performance (such as the stiffness) of the model and provides a more reliable structure.

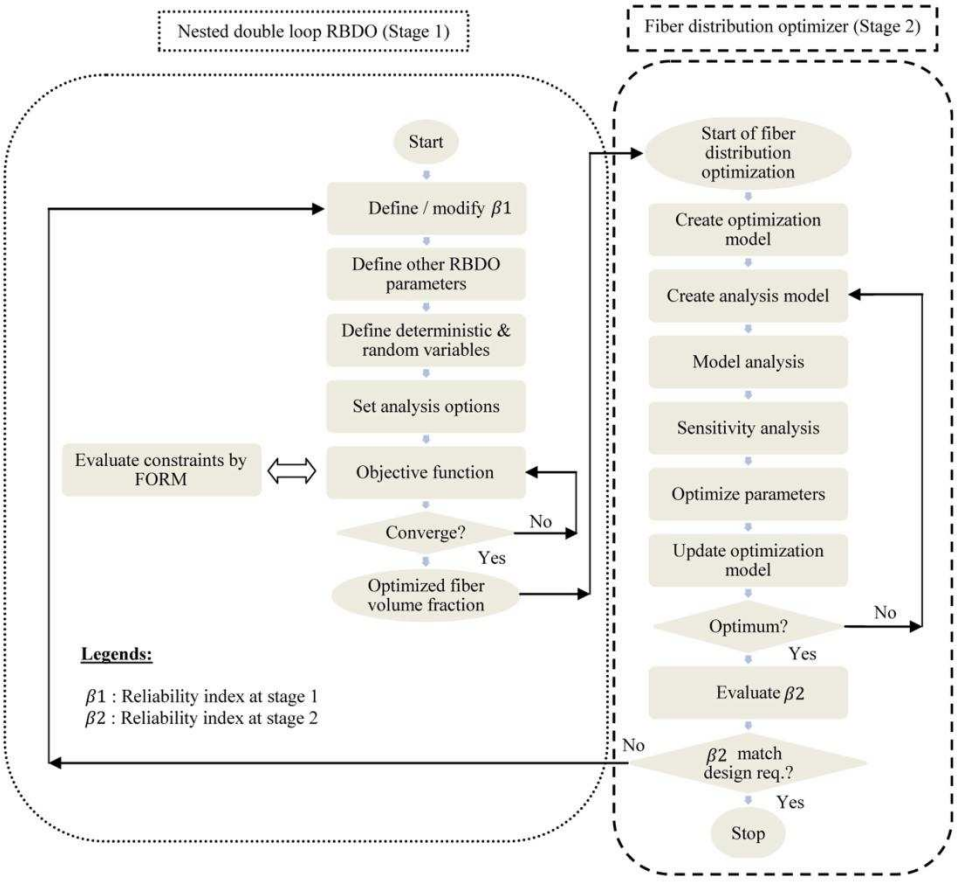

Fig.5. Double sequential stages optimization algorithm

It is however possible to implement concurrent approach for coupling stage 1 and stage 2. In the concurrent approach (Fig. 6) the fulfillment of the fiber distribution optimization before evaluation of LSF is necessary in every realization of stage 1. Thus, this alternative method is computationally expensive. To see more clearly the issue, we can assume that the computational parameter of total elapsed time (T_{total}) is proportional to the number of LSF call (n_1), each call run time (t_{LSF}) and the subtotal time required for fiber distribution optimization (t_2). Taking into account the above, for the sequential model the total time is proportional to the sum of the above mentioned times, i.e:

$$T_{total_{se}} \propto (n_1 \times t_{LSF} + t_2) \tag{29a}$$

while for concurrent model we have:

$$T_{total_{co}} \propto [n_1 \times (t_{LSF} + t_2)] \tag{29b}$$

as $n_1 > 1$, thus , $T_{total_{se}}$ is smaller than $T_{total_{co}}$. We can write:

$$(T_{total_{co}} - T_{total_{se}}) = \Delta T \propto [(n_1 - 1)t_2] \tag{30}$$

We can use a quantitative example in order to clarify the above issue. A simple case where t_2 and n_1 are equal to 20 minutes and 10 calls respectively, the present model is 180 minutes faster than the concurrent model. The computational advantage of this model is more evident when readers observe that t_2 and n_1 are considerably higher in real cases.

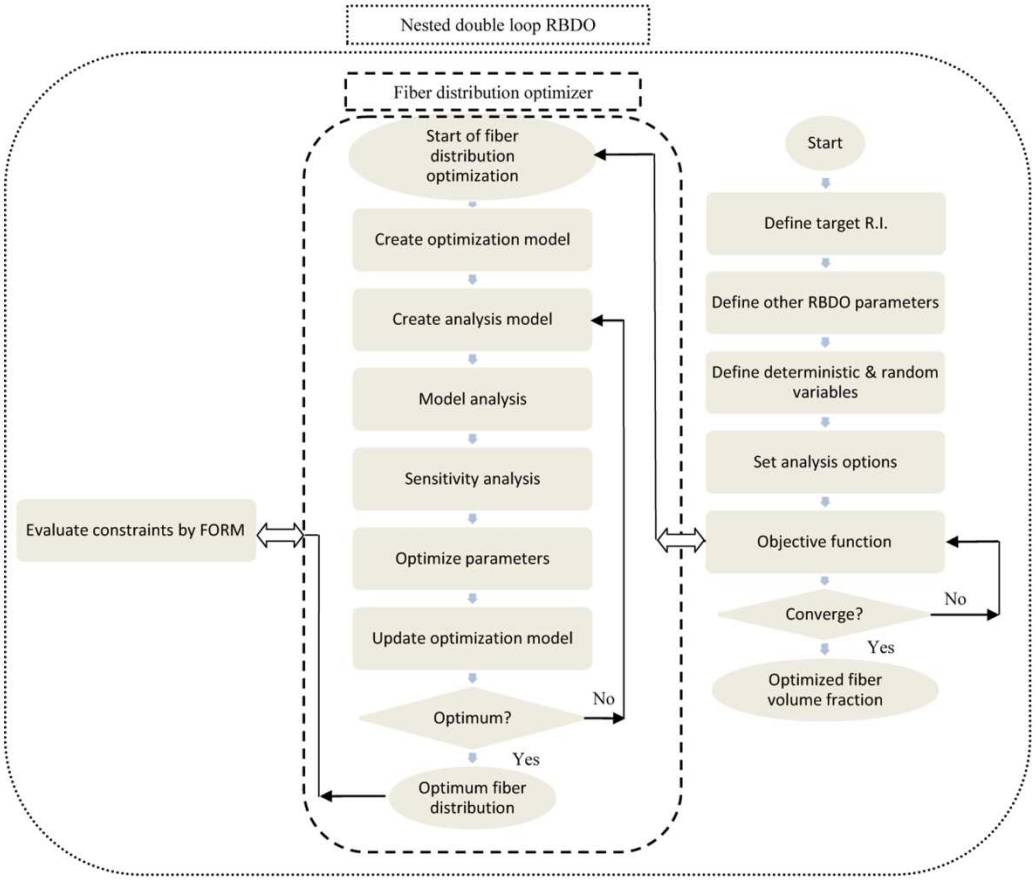

Fig.6. Concurrent optimization algorithm

6. Verification of the model through numerical examples

The aims of this section are firstly to verify the correctness and secondly to demonstrate the performance of the proposed model. Moreover the discussions related to the two presented examples will show how uncertainties influence the optimization of structural performance and how the presented algorithm can capture the effects of the uncertainties.

6.1 Cantilever beam under static loading, verification of the model

The first example involves a RBDO benchmark problem of a cantilever beam presented in [37] and shown in Fig.7. The beam length (L) is assumed to be equal to 100 inches with constant cross section area along its length.

The objective function corresponds to the minimization of the beam weight or equivalently, the cross section area ($w.t$). The limit state deals with the displacement at the free end of the beam, where the displacement attains its maximum value. F_x and F_y are independent random loads in x and y directions. R is random yield strength and E is Young's modulus. To verify the stochastic framework of the model, firstly we consider the analytical limit state function corresponding to the maximum displacement at the free end of the beam. Other design parameters are assumed exactly equal to those in the benchmark problem [37] and are summarized in Table-1.

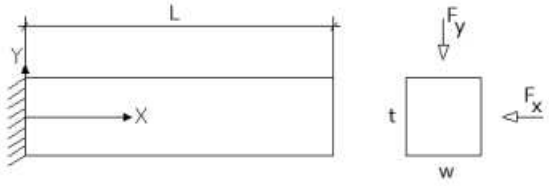

Fig.7. Schematic of the cantilever beam

Table-1. Benchmark problem definitions for cantilever beam under static loading condition

Parameter	L	R	F_x	F_y	E	w	t	β_1
Value	100	$\mu = 40000$ $\sigma = 2000$	$\mu = 40000$ $\sigma = 2000$	$\mu = 40000$ $\sigma = 2000$	$\mu = 29e6$ $\sigma = 1.45e6$	$\mu = 4$ $\sigma = 0.001$	$\mu = 4$ $\sigma = 0.001$	3
Type	D	N	N	N	N	N	N	D

$L: Length,\ R: yield\ strength,\ F_x, F_y: load,\ E: Young's\ Modulus,\ w, t: width, thickness$

$D: deterministic, N: normal\ distribution, \mu: mean\ value, \sigma: standard\ deviation, \beta: Reliability\ Index$

Table-2 compares the obtained results and the benchmark ones and shows that there is an agreement between them.

Table-2. RBDO results using analytical limit state

Method	w	t	$F = w.t$
Benchmark [37]	2.700	3.410	9.206
Present Model	2.702	3.408	9.206

$w, t: width, thickness \qquad F: Objective\ function$

In the next step we set the off-plane load (F_x) equal to zero in order to solve the problem in 2-D space while keeping the beam depth equal to unity. Results which are obtained by using two different limit state functions (i.e. analytical formula and those calculated by finite elements) are compared with each others in Table-3. Once again a good conformity was obtained.

Table-3. RBDO results using FEM limit state

Method for evaluation of LSF	w	t	$F = w.t$
Analytical	1	4.0095	4.0095
FEM (NURBS)	1	4.0094	4.0094

$w, t: width, thickness$ $F: Objective\ function$

6.2 Beam under three-point bending

In the present example the first objective function is to find the optimal fiber volume while the limit state is the deflection at mid of the beam must be smaller than an admissible value. Fig.8 shows the schematic view of the problem and Table-4 includes the design parameters.

Table-4. Problem definitions of the beam under static loading

Parameter	L_x	L_y	E_m	E_f	ν	P	LSF	β_1	$Obj.Func.$
Value	5	1	$\mu = 20$ $\sigma = 5$	$\mu = 200$ $\sigma = 50$	0.1	$\mu = 1000$ $\sigma = 250$	Max. Deflection $4e^{-3}$	3	Fiber volume fraction
Type	D	D	N	N	D	N	D	D	D

$Length: (M),\ E: (MPa),\ P: Applied\ load\ (N),\ \nu: Poisson\ ratio,\ m: matrix,\ f: fiber$

$D: deterministic, N: normal\ distribution, \mu: mean\ value, \sigma: standard\ deviation\ \ \beta_1: Reliability\ Index$

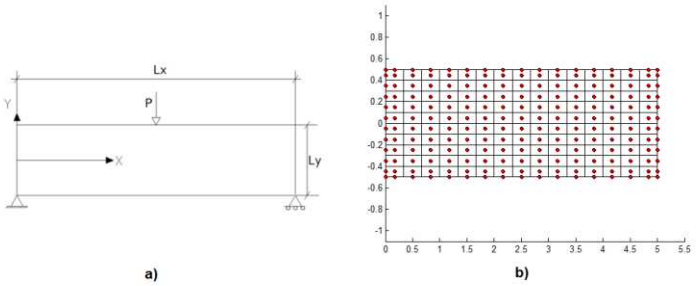

Fig.8. Geometry (a) and FE mesh with control points indicated by dots (b) of a three-point bending beam

Fig.9 presents optimal values of fiber volume fraction for the beam with homogeneously distributed fibers versus the different maximum allowable deflection at mid of the beam and for

different reliability indices. A mesh with 91 control points has been used to reduce computational cost. As expected, either demanding smaller beam deflection or greater reliability index for the beam, yield to increase in fiber volume fraction of the FRC beam. The figure also depicts that for large reliability indices (here 4 and 5) and when there is a small allowable beam deflection (here 5 mm), the obtained fiber contents are approximately the same.

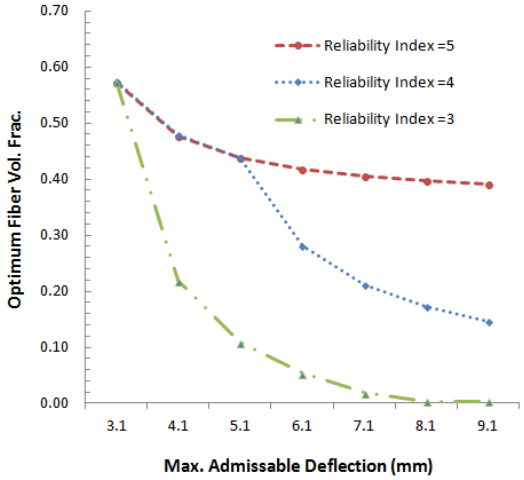

Fig.9. Fiber volume fraction versus change in maximum admissible deflection for different R.I.

Results of RBDO by using 1225 control points, which represents 41×20 mesh sizes, are plotted in Fig.10. For this (or higher) number of control points, the numerical solutions of the LSF have been verified to converge to the exact solution.

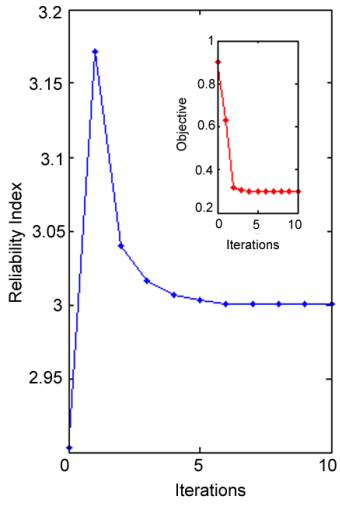

Fig.10. RBDO results of a three-point bending beam using 1225 control points

Fig.11 compares the obtained values related to the assumed objective function for different numbers of control points (mesh sizes). As can be observed, the deviation between the obtained optimal fiber volume fractions by using 1225 or 325 control points is equal to 0.03 (i.e. 3%) but the computational time is reduced to be approximately less than one tenth. This fact underlines NURBS smooth and quick convergence characteristics which yield to noticeable saving in the time of the computation. In RBDO problem, LSF which depends on FE model results, should be evaluated many times. So, any reduction in its calculation time will significantly reduce the total elapsed time. Admittedly, this time saving is justified only in the case that accuracy of the results is also maintained. This takes place in the presented model while using coarse NURBS mesh for the evaluation of LSF, slightly changes in the accuracy of the results and leads to a significant decrease in RBDO computational time.

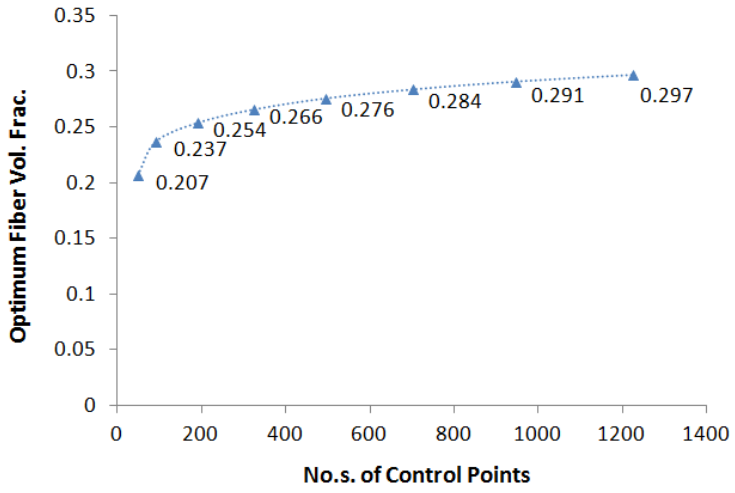

Fig.11. RBDO results versus number of control points (mesh size)

Once the optimal fiber content (by assuming $\beta_1 = 3$) is obtained (Fig.12 (a)), the second module optimizes the fiber distribution through the structure (Fig.12 (b)), with the aim to minimize the structural compliance. 703 control points are used for obtaining shown results. The obtained target reliability index at the end of stage 2 is $\beta_2 = 7.66$. This increase in reliability index is due to the effect of fiber distribution optimization on increasing the structural stiffness which consequently decreases the deflection of the structure. It is also noteworthy to mention that in this case the standard deviations of random variables are according to Table-4. If they are

decreased to 70% and 40% of the current values without any change in other design parameters, since required fiber volume fractions decrease, the target reliability indices are also decreased to $\beta_2 = 6.65$ and $\beta_2 = 4.81$, respectively. Thus, we can conclude that fiber distribution optimization is more influential on increasing the reliability of the structure with higher level of uncertainties.

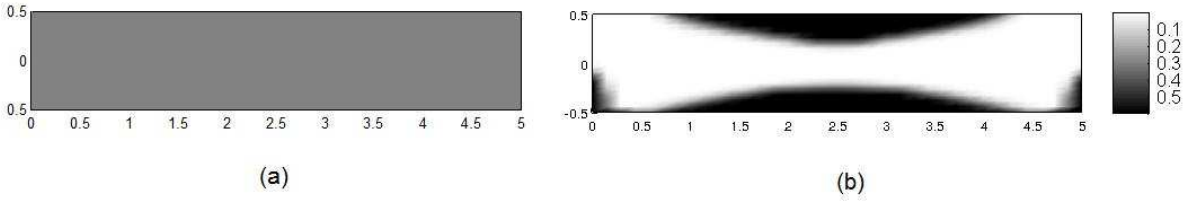

Fig.12. Three point bending wall beam problem using 703 control points with (a) homogenized fiber distribution and $\beta_1 = 3$, (b) optimized fiber distribution and $\beta_2 = 7.66$

6.3 Square plate with a central circular hole under tension

The classical problem of a square plate with a central hole under constant distributed edge load is assumed as the second example. Considering the double symmetry of the problem, just one quarter of the plate is modeled. Fig.13 (a) and (b) show the analysis model and the FE domain discretization. Table-5 shows the design parameters. The problem of obtaining optimal fiber volume fraction and distribution in order to have a reliable structure with limited deflection, is solved by using quadratic NURBS meshes.

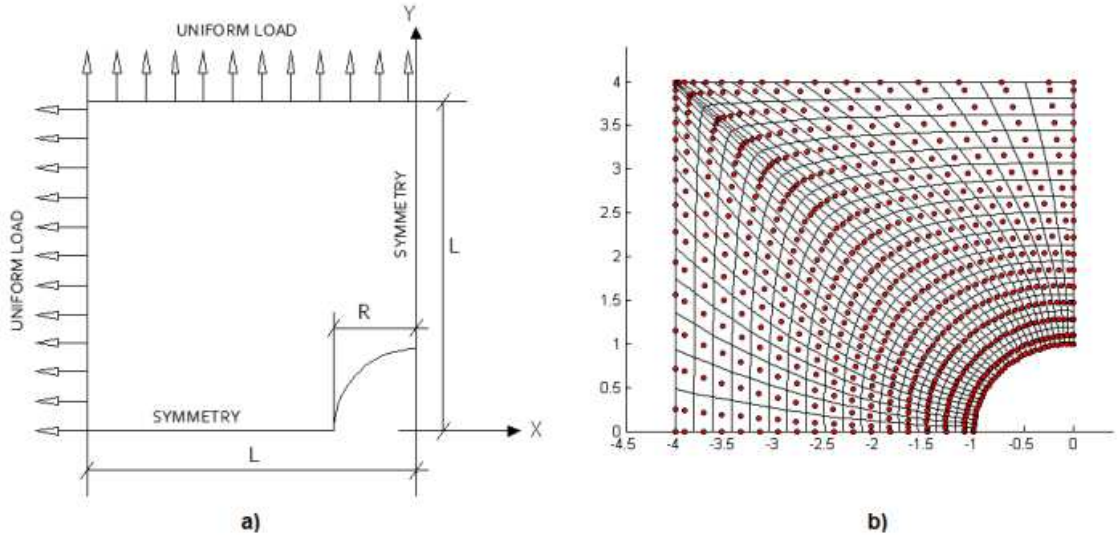

Fig.13. Square plate with central hole (a) schematic view, (b) mesh with control points

Table-5. Problem definitions, Square plate with central hole

Parameter	L	R	E_m	E_f	ν	P	LSF	β_1	$Obj.Func.$
Value	4	1	$\mu = 20$ $\sigma = 2$	$\mu = 200$ $\sigma = 20$	0.1	$\mu = 510$ $\sigma = 20,30,40,50$	Max. Deflect $(6e^{-8})$	3	Fiber volume
Type	D	D	N	N	D	N	D	D	D

$Length: (M),\ E: (GPa),\ P: Applied\ load\ (N/m),\ \nu: Poisson\ ratio,\ m: matrix,\ f: fiber$

$D: deterministic, N: normal\ distribution, \mu: mean\ value, \sigma: standard\ deviation, \beta_1: Reliability\ Index$

Firstly, all the design parameters are considered as deterministic values, except the applied load which is considered as a random variable with different standard deviations. Obtained optimal fiber contents (by using 612 control points) are plotted versus the values of standard deviation of the applied load in Fig.14.

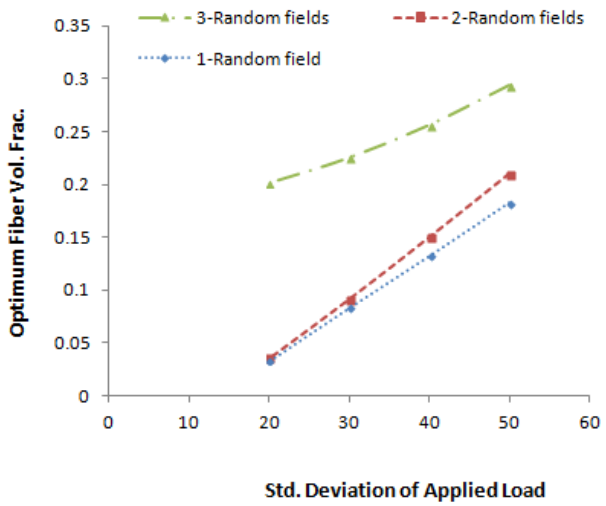

Fig.14. Optimal fiber volume fraction versus standard deviation of applied load considering $\beta_1 = 3$ for 1- Random field (load), 2-Random fields (load+E_f) and 3-Random fields (load+$E_f + E_c$)

As can be seen, an increase in the standard deviation of the applied load (which means an increase in the uncertainty of the system) needs more fiber content. The system uncertainty will increase more when we consider the Young's modulus of fiber as another random field (i.e. 2-Random fields) and even more when the Young's modulus of the matrix material is also considered as a random variable (i.e. 3-Random fields). In the case where only the applied load is assumed as a random variable (with mean value equal to $510\ N/m$ and standard deviation

equal to 50), the optimal fiber volume fraction is equal to 0.183. When E_f is also considered as a random variable, the optimal fiber volume is equal to 0.21. When E_m is not deterministic any more, the optimal fiber volume becomes 0.294. As can be seen, by increasing the number of random variables while keeping constant the reliability index (i.e. $\beta_1 = 3$), the required fiber volume fraction increases. Alternatively, for a constant fiber volume fraction, if the number of uncertain variables of the problem increases, the reliability of the system decreases.

Using 612 control points, optimal fiber distribution leading to the minimum structural compliance is plotted in Fig.15. Considering $\beta_1 = 3$, the target reliability index for this pattern of fiber distribution gives the value of $\beta_2 = 4.1$. Changes in $\beta_1$will result in different values of β_2, for example for $\beta_1 = 2.5$ and $\beta_1 = 3.5$ the target reliability indices correspond to $\beta_2 = 3.78$ and $\beta_2 = 4.36$, respectively.

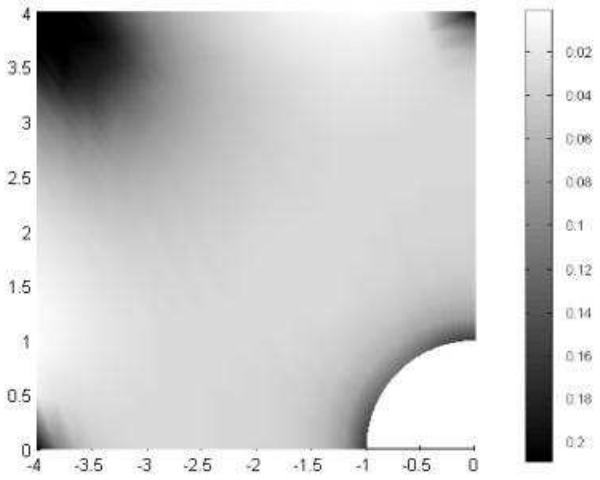

Fig.15. Optimal distribution of fibers with volume fraction 0.294 of plate with central hole subjected to constant loading, target reliability index $\beta_2 = 4.1$ (result for 612 control points)

7. Conclusions

An efficient sequential algorithm for finding the optimal fiber volume fraction and its distribution in structures made of FRC materials is presented. To overcome the cumbersome computational burden in stochastic optimization problems, finding the optimal fiber volume fraction and fiber distribution are performed sequentially, not concurrently. This technique along with using NURBS finite elements, allows us to get a noticeable reduction in the computational

cost, without a noticeable loss in accuracy of the results. Assuming a random orientation of fibers in the matrix, in the first optimization module (i.e. finding the optimal fiber volume fraction) uncertainties in the parameters (such as constituent's materials and loading) are fully addressed and LSF is evaluated by using FORM. In the second module (i.e. fiber distribution optimization) a NURBS surface which smoothly defines the fiber distribution pattern, is adopted. The presented numerical examples show as an increase in model uncertainties gives rise to unreliability of the system. More specifically, either the rise in the number of uncertain fields in the problem or the increase in the standard deviation of random variables needS more fiber content. It can be also concluded that when there is a higher level of uncertainties in design parameters, the fiber distribution optimization is more influential on increasing the reliability of the structure. Developing the present methodology from current serviceability to collapse limit states, where the FRC structure loses its integrity and also multi component system instead of single piece structure would be interesting issues for industrial applications and will provide the scope of our future studies.

Acknowledgments:

This work was supported partially by Marie Curie Actions under the grant IRSES-MULTIFRAC and German federal ministry of education and research under the grant BMBF SUA 10/042. Nachwuchsförderprogramm of Ernst Abbe foundation, the National Basic Research Program of China (973 Program: 2011CB013800), Program for Changjiang Scholars and Innovative Research Team in University (PCSIRT, IRT1029), Pujiang Program (12PJ1409100) and the research support provided by the Italian Ministry for University and Technological and Scientific Research (MIUR) are also acknowledged.

References:

1- L.Y.Woo, S.Wansom (2005) Characterizing fiber dispersion in cement composites using AC-Impedance Spectroscopy. Cement and Concrete Composites 27(6): 627-636.
2- B.Y.Lee, J.K.Kim (2009) Quantitative evaluation technique of Polyvinyl Alcohol (PVA) fiber dispersion in engineered cementitious composites. Cement and Concrete Composites 31(6): 408-417.
3- Z. Yan, Duan Yuexin (2009) The dispersion of SWCNTs treated by dispersing agents in glass fiber reinforced polymer composites. Composites Science and Tech. 69(13): 2115-2118.

4- Chuang Wang, Ke-Zhi Li (2008) Effect of carbon fiber dispersion on the mechanical properties of carbon fiber-reinforced cement-based composites. Material Science and Engineering 487(1-2): 52-57.
5- D.M Scott. (1997) Nondestructive analysis of fiber dispersion and loading. Composites Part A: Applied Science and Manufacturing 28(8): 703-707.
6- Dongyang Wu, Dachao Gao (2008) X-ray ultramicroscopy: A new method for observation and measurement of filler dispersion in thermoplastic composites. 68(1): 178-185.
7- J. Huang, R.T. Haftka (2005) Optimization of fiber orientations near a hole for increased load-carrying capacity of composite laminates. Struct Multidisc Optim 30: 335-341.
8- R. Brighenti (2005) Fiber distribution optimization in fiber-reinforced composites by a genetic algorithm. Composite Structures 71: 1-15.
9- H. Ghasemi, R. Brighenti, X. Zhuang, J. Muthu, T. Rabczuk (2014) Optimization of fiber distribution in fiber reinforced composite by using NURBS functions. Computational Material Science 83: 463–473
10- Di Sciuva M, Lomario D. (2003) A comparison between Monte Carlo and FORMs in calculating the reliability of a composite structure. Compos Struct 59(1): 155–62.
11- P.B.Thanedar, C.C.Chamis (1995) Reliability considerations in composite laminates tailoring. Computer and struct. 1995 54(1): 131–139.
12- C. Jiang, X. Han, G.P. Liu (2008) Uncertain optimization of composite laminated plates using a nonlinear interval number programming method. Computer and struct. 86: 1696–1703.
13- H.M.Gomes, A.M.Awruch (2011) Reliability based optimization of laminated composite structures using genetic algorithms and Artificial Neural Networks. Structural safety 33: 186–195.
14- C. C. Antonio, L. N. Hoffbauer (2009) An approach for reliability-based robust design optimization of angle-ply composites. Composite structure 90: 53–59.
15- Y.J. Noh, Y.J. Kang. (2013) Reliability-based design optimization of volume fraction distribution in functionally graded composites. Comp. Material Science 69: 435–442.
16- R. Brighenti (2004) Optimum patch repair shapes for cracked members. Int. J. of Mech. Mat. in Des. 1(4): 365-381.
17- R. Brighenti, A. Carpinteri, S. Vantadori (2006) genetic algorithm applied to optimization of patch repairs for cracked plates. Comp. Meth. App. Mech. Eng. 1960: 466-475.
18- R. Brighenti (2007) Patch repair design optimization for fracture and fatigue improvements of cracked plates. J. of Sol. Struct. 44(3-4): 1115-1131.
19- S. Kulasegaram, BL. Karihaloo, A. Ghanbari (2011) Modeling the flow of self-compacting concrete. International Journal for Numerical and Analytical Methods in Geomechanics. 35 (6): 713-723 ISSN 0363-9061 10.1002/nag.924
20- S. Kulasegaram, BL. Karihaloo (2012) Fibre-reinforced, self-compacting concrete flow modeled by smooth particle hydrodynamics. Proceedings of the ICE Engineering and Computational Mechanics. 166 (1): 22-31 ISSN 1755-0777 10.1680/eacm.11.00004
21- Hashin Z. (1962) The elastic moduli of heterogeneous materials. J Appl Mech. 29: 143-150.
22- Hashin Z. and S. Shtrikman (1963) A variational approach to the theory of elastic behavior of multiphase materials. J. Mech. Phys. Solids 11: 127-140

23- B.Paul (1960) Prediction of elastic constants of multiphase materials. Transactions of the Metallurgical Society of AIME p. 36-41.
24- Hill R. (1965) A self-consistent mechanics of composite materials. J. Mech. Phys. Solids 13: 213-222.
25- Mori T, Tanaka K. (1973) Average stress in matrix and average elastic energy of materials with mis-fitting inclusions. Acta Metal 21: 571-583
26- R. Brighenti (2012) A micromechanical model and reinforcing distribution optimization approach for fiber-reinforced materials. In: Qingzheng (George) Cheng (ed) Fiber Reinforced Composites, Nova Science Publishers, Inc., Hauppauge, NY, pp 527-569.
27- R. Brighenti (2004) A mechanical model for fiber reinforced composite materials with elasto-plastic matrix and interface debonding. Int. J. of Computational Materials Science 29:475-493.
28- R. Brighenti (2004) Numerical modeling of the fatigue behavior of fiber-reinforced composites. Int. J. of Composite Part B: Engineering 35(3): 197-210
29- R. Brighenti, D. Scorza (2012) A micro-mechanical model for statistically unidirectional and randomly distributed fiber-reinforced solids. Mathematics and Mechanics of Solids17(8):876–893.
30- Ditlevsen O, Madsen H (1996) Structural reliability methods. John Wiley & Sons, UK
31- Hasofer, A.M. and Lind N. (1974) An Exact and Invariant First-Order Reliability Format. Journal of Engineering Mechanics ASCE 100: 111–121.
32- M.Chiachio, J.Chiachio, G.Rus (2012) Reliability in composites - A selective review and survey of current development. Composites 43(B): 902-913.
33- Yan-Gang Zhao, Tetsuro Ono (1999) A general procedure for first/second-order reliability method (FORM/SORM). Structural safety 21: 95–112.
34- Kiureghian A.D. (2006) Structural reliability software at the university of California, Berkeley. Struct Safe 28: 44-67
35- J.A. Cottrell, T.J.R. Hughes, Y.Bazilevs (2009) Isogeometric Analysis towards integration of CAD and FEA. Wiley, UK
36- Zhou M., Rozvany GIN (1991) The COC algorithm part II: topological, geometry and generalized shape optimization. Comput. Methods Appl. Mech. Eng. 89: 197-224.
37- V. Togan, A. Daloglu (2006) Reliability and reliability based design optimization. Turkish J. Eng. Env. Science 30: 237-249.